

# Spectral based Analysis of Airborne Hyperspectral Remote Sensing Image for Detection of *Ganoderma* Disease in Oil Palm

Mohamad Anuar Izzuddin<sup>1</sup>, Abu Seman Idris<sup>1</sup>, Nor Maris Nisfariza<sup>2</sup>, Bahrom Ezzati<sup>2</sup>

<sup>1</sup>Malaysian Palm Oil Board (MPOB), 6, Persiaran Institut, Bandar Baru Bangi, 43000 Kajang, Selangor, Malaysia

<sup>2</sup>Department of Geography, Faculty of Arts and Social Sciences, University of Malaya, 50603 Kuala Lumpur, Malaysia

**Abstract:** In this study, the AISA Eagle airborne hyperspectral image was used to detect and map three levels of BSR disease severity in oil palm plantation using five spectral indices (SI) and four Continuum Removal (CR). The accuracy of the SI and CR was then assessed using confusion matrix and t-test. The results revealed that only two SI, i.e. Simple Ratio Index (SRI) and Enhanced Vegetation Index (EVI) had moderate capability for the detection of BSR disease in oil palm. SRI showed moderate accuracy of 44.4% compared to EVI with 40.7% accuracy; while the other three SIs had poor accuracy (<40%). The results indicated that the SIs generated from airborne hyperspectral image had low accuracy for detection of BSR disease in oil palm. Meanwhile, the results of t-test of the four CR. showed significant distinctions between all severity classes in the 500 nm absorption features for young oil palm. Further studies must be conducted to develop specific spectral analysis method for BSR disease detection in oil palm using airborne hyperspectral remote sensing.

**Keywords:** hyperspectral, *Ganoderma*, continuum removal, spectral indices.

## 1. Introduction

The palm oil industry is one of Malaysia's key socio-economic drivers and important for the growth of the country but basal stem rot disease (BSR) caused by *Ganoderma spp.* had destroyed oil palm and resulted profit reduction to Malaysian economy [1]. A fast and accurate method for this disease detection is required to prevent loss [2]. The *Ganoderma* disease incidences have been reported to occur in oil palm cultivated in all types of soil; coastal, inland, peat and lateritic[3]. The most aggressive *Ganoderma* species that causes BSR disease is *Ganoderma boninense* [4]. The disease spreads by the *Ganoderma* mycelium that grows along the infected root and eventually reaches the bole region of the palm. The *Ganoderma* disease shortens the life span of the oil palm and affecting the yield of the fresh fruit bunches [5].

Several technologies implemented to detect *Ganoderma* disease on individual oil palm have been developed. They are *Ganoderma* Selective Medium (GSM)[6], Polyclonal Antibodies Enzyme-Linked Immunosorbent Assay (PAbS-ELISA)[7][8]), Multiplex PCR-DNA Kit [9], and GanoSken Tomography [10]. The disadvantages are that these detection technologies required a lot amount of labour, cost and time. The availability of airborne hyperspectral remote sensing can provide wide aerial view over oil palm plantation compared to the individual oil palm detection techniques [2]. Airborne hyperspectral imaging utilises camera on airborne platform that acquires images in many narrow, contiguous spectral bands throughout the visible, near infrared, mid infrared and thermal infrared portions of the spectrum [11]. [12] used CR to characterise the wavelengths suitable for detection of brown spot disease on rice and found that the suitable ranges were 401 nm – 530 nm, 550 nm – 730 nm, 498 nm and 678 nm. Studies by [13] used hyperspectral remote sensing in detecting stress caused by late blight disease in tomatoes from airborne visible infrared imaging spectrometer (AVIRIS) and suggested several SIs suitable for the disease detection. The objective of our study was to assess capability of SI and CR to differentiate different level of *Ganoderma* disease severity in oil palm using airborne hyperspectral imagery.

## 2. Methodology

### 2.1. Study Area and Hyperspectral Airborne Image Acquisition

The study area was located in an oil palm plantation located at Seberang Perak, Perak, Malaysia (4° 6' 42" N, 100° 53' 12" E) (Figure 1a) with annual precipitation of 2256 mm and temperature between 24°C - 34°C. The airborne hyperspectral imagery was acquired in 20 October 2008 over a portion of oil palm plantation (5 years old palm) where *Ganoderma* disease incidence was reported. The Airborne Imaging Spectrometer for Applications (AISA) (Figure 1b) is a pushbroom camera that covered spectrum range from 400 to 970 nm with spectral intervals of approximately 4.6 nm consisted of 128 bands. The altitude during image acquisition was set to 1 km above sea level. Caligeo and ENVI QUAC function in ENVI 4.8 software was used for pre-processing of the image [14].

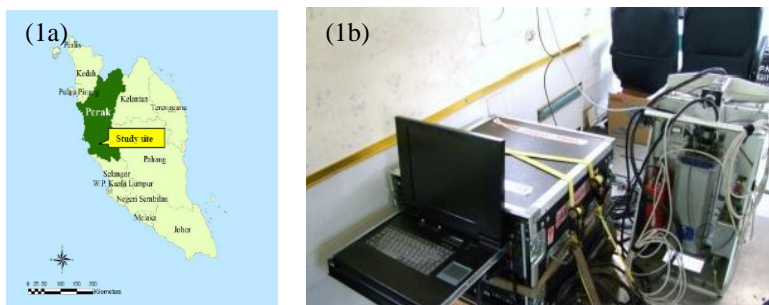


Fig. 1: a) Study site of oil palm plantation, Seberang Perak, Malaysia; and b) The AISA airborne hyperspectral system

### 2.2. The *Ganoderma* Disease Ground Census

The ground data consisted of *Ganoderma* disease severity levels and was prepared through visual inspection of oil palm in the study area. The oil palms were selected and categorised based on description as presented in Table 1. The GSM was used to confirm the presence of *Ganoderma* disease in oil palm.

TABLE I: *Ganoderma* disease severity levels

Disease Severity	Description	Visual Assessments
T1	Uninfected palm and GSM negative.	Looks healthy, no foliar symptoms and absence of white mycelium or fruiting body ( <i>Ganoderma</i> ) at the stem base.
T2	Infected palm with <i>Ganoderma</i> fungus without any foliar symptoms but with small white button or fruiting body at the stem base, GSM positive.	Looks healthy, no foliar symptoms but presence of small white button and/or fruiting body ( <i>Ganoderma</i> ) at stem base.
T3	Infected palm with <i>Ganoderma</i> fungus with foliar symptoms and white mycelium or fruiting body at stem base, and GSM positive.	Yellowing or drying of some leaves. Three or more remain as unopened spears. Rupture of older fronds. Presence of small white button and/or fruiting body ( <i>Ganoderma</i> ) at the stem base.

### 2.3. Spectral Indices (SIs) and Continuum Removal (CR) Processing

The SIs is a combination of area reflectance at two or more wavelengths designed to highlight a particular property of vegetation to describe plant foliage. The hyperspectral image was transformed into SIs using the Vegetation Analysis Tool provided in ENVI 4.8 Software. Five SIs and four CR were used is showed in Table 2 and Table 3.

TABLE II: List of Spectral Indices (SIs)

No.	Spectral Indices (SIs)	Formulae
1.	Normalised Difference Vegetation Index (NDVI)	$NDVI = \frac{\rho_{NIR} - \rho_{RED}}{\rho_{NIR} + \rho_{RED}}$
2.	Simple Ratio Index(SRI)	$SR = \frac{\rho_{NIR}}{\rho_{RED}}$
3.	Enhanced Vegetation Index (EVI)	$EVI = 2.5 \left( \frac{\rho_{NIR} - \rho_{RED}}{\rho_{NIR} + 6\rho_{RED} - 7.5\rho_{BLUE} + 1} \right)$
4.	Vogelmann Red Edge Index 1 (VREI 1)	$VOG1 = \frac{\rho_{740}}{\rho_{720}}$
5.	Carotenoid Reflectance Index 2 (CRI 2)	$CRI2 = \left( \frac{1}{\rho_{510}} \right) - \left( \frac{1}{\rho_{700}} \right)$

TABLE III: List of Continuum Removal (CR)

No.	Continuum Removal (CR)	Formulae
1.	Continuum-removed reflectance (CRR)	$CRR = R/CR$
2.	Band Depth (BD)	$BD = 1 - CRR$
3.	Normalised Band Depth (NBD)	$NBD = BD/BD_c$
4.	Band Depth Normalised to Area (BDNA)	$BDNA = BD/\Sigma BD$

The five SIs were selected based on literature review on potential application of these SIs for vegetation stress and disease [15]. The NDVI was introduced by [16] separates green vegetation from its background soil brightness. NDVI values are ranging from -1 to 1; with 0 and negative value representing non-vegetated areas.

The SRI is constructed as a ratio to minimised illumination difference due to topography. However, SRI is susceptible to division by zero errors and resulting measurement scale is not linear [17].The EVI is a modified NDVI with a soil adjustment factor L and two coefficients, C1 and C2, which describe the usage of the blue band in correction of the red band for atmospheric aerosol scattering [18]. The VREI 1 is a narrowband reflectance measurement that is sensitive to the combined effects of foliage chlorophyll concentration, canopy leaf area and water content. The values of this index range from 0 to 20 [19].The CRI 2 is as reflectance measurement which is sensitive to carotenoid pigments in plant foliage. Higher CRI 2 value means greater carotenoid concentration relative to chlorophyll [20].

Meanwhile, CR is a method that normalized reflectance spectra from image to compare individual absorption features from a common baseline. The continuum is defined as the convex hull fit over the top of each line segments to the spectrum maxima and the continuum is removed by dividing the convex hull to the original spectrum [21]. We used four CR which are: 1) Continuum Removed Reflectance (CRR); 2) Band Depth (BD); 3) Normalised Band Depth (NBD); and 4) Band Depth Normalised to Area (BDNA) (Table 3).

## 2.5. Output Assessment

Confusion matrix used to calculate overall accuracy of SIs image classification[22]. Kappa value was also calculated to define the good and poor accuracy classes (Table 4) [23].

TABLE IV: Interpretation of kappa values with respect to classification accuracy classes

Kappa value	Classification accuracy class
<0	Poor
0.01-0.20	Slight
0.21-0.40	Fair
0.41-0.60	Moderate
0.61-0.80	Substantial
0.81-0.99	Good

Meanwhile the CR outputs were assessed using t-test. The t-test compared differences between the sample means by computing the t-statistic and the degrees of freedom for choosing the tabulate t-value. The t-test analysis was adopted by [24] in discriminating shrubs and tree species from hyperspectral SIs.

### 3. Results and Discussions

The AISA airborne images were processed using Caligeo software for geometric and radiometric correction into an orthoimage and converted to orthoimage mosaic. The study area is highlighted in Figure 3.

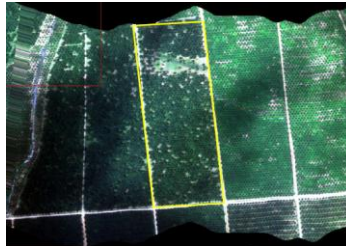


Fig. 3: AISA Eagle hyperspectral image of oil palm plantation. The yellow box indicates the study area.

#### 3.1. Classification of Spectral Indices

The five SIs were classified using the density slicing method into T1, T2, T3 and non-vegetated area. Several iterations of density slicing were conducted during the classification process. The iterations were conducted to determine the suitable ranges of SIs values that represented the disease severity levels. Table 5 showed the SIs values for T1, T2 and T3 and non-vegetated area.

TABLE V: Spectral Indices value for *Ganoderma* disease severity levels

Disease Severity Level/Non-Vegetated Area	Vegetation Index / Value				
	NDVI	SRI	EVI	VREI1	CRI2
T1	0.9 - 1.0	12.6 - 21.0	0.7 - 1.0	2.4 - 3.1	9.0 - 54.5
T2	0.7 - 0.8	10.0 - 12.5	0.4 - 0.7	2.2 - 2.4	8.5 - 10.0
T3	0.4 - 0.6	2.0 - 10.0	0.1 - 0.4	1.5 - 2.2	2.0 - 8.5
Non vegetated	0.0 - 0.3	0.0 - 2.0	0.0 - 0.1	0.0 - 1.5	0.0 - 2.0

Table 5 provides the values of SIs for each disease category. Higher values means healthy oil palms and the lowest resembled the non-vegetated areas. The SIs images were then classified into T1, T2, T3 and non-vegetated area (Table 6). The output images were then verified with the points from ground census map to assess the accuracy using confusion matrix. The difference between observed and expected locations of T1, T2 and T3 was measured in overall percentage of accuracy and also their kappa values. Table 6 shows the classification output of the SIs. The small dots overlaid on the output are the location of T1, T2 and T3 training data points. SRI gave the highest accuracy (44.4%) followed by EVI (40.7%). The VREI 1 and CRI 2 gave the same percentage accuracy at 37.0% while the accuracy for NDVI was only 33.3%. The Kappa values assisted the interpretation of accuracy. The highest Kappa value was for SRI (0.43) followed by EVI (0.41) indicating a moderate classification accuracy while VREI 1 and CRI 2 shared the same Kappa value (0.056), and NDVI showed the lowest Kappa value (0.000) which reflected a poor classification accuracy.

Low, positive values of NDVI (0.3 to 0.7) generally correspond to infected palms, while the middle range (0.7 to 0.8) represent infected but looking healthy palms, NDVIs values of 0.8 to 1.0 indicate healthy palms. Our results were contrary to the findings obtained by [25] who reported that NDVI had a high accuracy (81%) for detection of wheat rust disease. The difference may have resulted from the quality of image acquired and the radiometric properties the difference of image acquisition approach. Results by [26] also were not similar with our results which suggested that NDVI, SRI, and VREI 1 had high accuracy from 78%-82% and different with our findings where the SIs only cover accuracy from 33.3% to 44.4%. [26] only studied the difference between healthy and diseased oil palms, while we conducted a study that attempted to differentiate three levels of *Ganoderma* disease severity. [26] suggested that modification of the SIs is required in order to differentiate between the *Ganoderma* disease severity levels. Their results accuracy were not yet tested on airborne hyperspectral images.

TABLE VI: Results of Spectral Indices classification

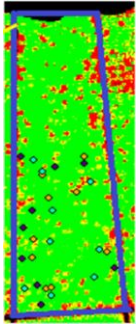
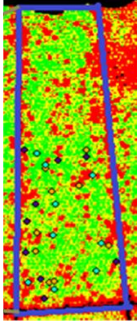
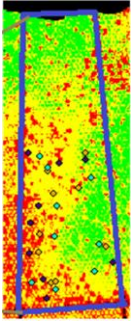
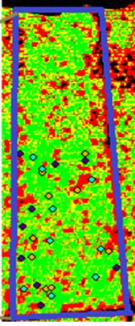
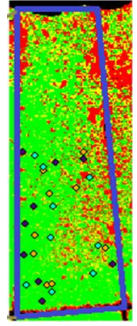
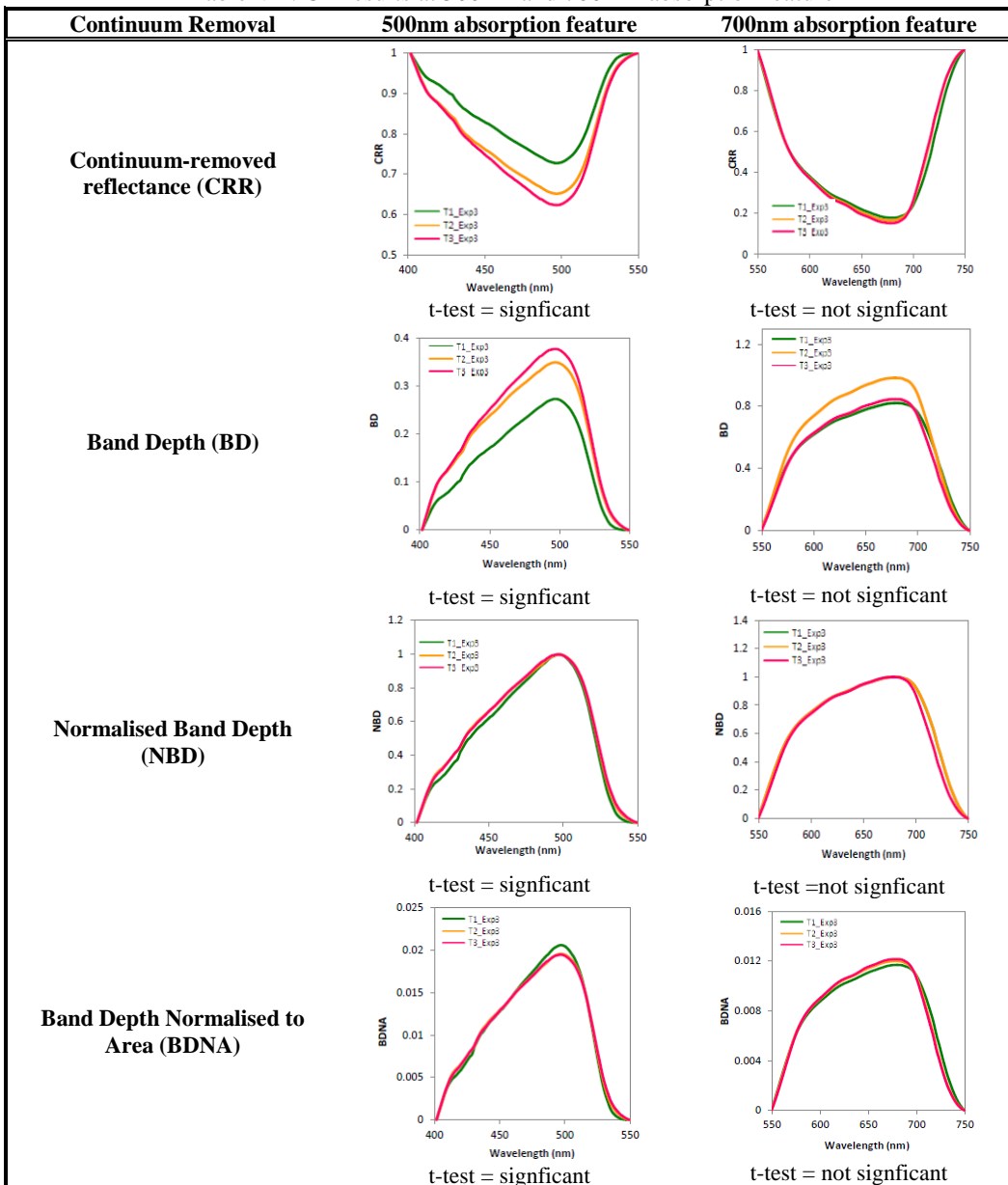
Vegetation Index	NDVI	SRI	EVI	VREI 1	CRI 1
<b>Classification Output</b>					
<b>Legend</b>	<ul style="list-style-type: none"> <li><span style="color: green;">■</span> T1</li> <li><span style="color: yellow;">■</span> T2</li> <li><span style="color: red;">■</span> T3</li> <li><span style="color: black;">■</span> Non-vegetated</li> </ul>				
<b>Overall Accuracy (%)</b>	33.3	44.4	40.7	37.0	37.0
<b>Kappa</b>	0.000	0.43	0.41	0.056	0.056

Table VII: CR results at 500nm and 700 nm absorption feature



[11] and [15] had studied several SIs for *Ganoderma* disease detection using airborne hyperspectral images and their results concurred with our results. [11] suggested that the SIs required modification by implementation of significant wavelengths into the SIs formulae and applied the continuum removal to the spectral signatures of the *Ganoderma* disease severity. Furthermore, [2] and [27] had develop specific SIs for detection of *Ganoderma* disease in oil palm using field spectroscopy but the results cannot be compared directly with our study because the results have not yet been tested on airborne hyperspectral image. Our study concluded that SRI had the highest accuracy followed by EVI, VREI 1, CRI 2 and NDVI. However, the accuracy of the SIs were moderate and poor and modification is needed to improve the results.

For CR analysis, two continuum removed regions were selected at 500 nm absorption feature (400 – 500 nm) and 700 nm absorption feature (550 – 750 nm). Analysis using visual inspection and t-test on the 500 nm absorption feature showed that there are significant difference between T1, T2 and T3 by using the four CR but at 700 nm absorption features the results showed that all four CR showed less significant difference between T1, T2 and T3 and all CR at 700nm absorption feature show no significant difference between T2 and T3 (Table 7).

#### 4. Conclusions and Recommendations

Our study reviewed five SIs and four CR for detection of different *Ganoderma* disease severity levels. Density slicing classification technique with several iterations was used to classify the SIs images into T1, T2 and T3 and t-test was conducted for CR analysis. The results showed that none of the SIs had good accuracy while only CR on 500 nm absorption features showed significant difference between T1, T2 and T3. The results suggested that the SIs used in this study were not very suitable for detection of *Ganoderma* disease in oil palm. Future works using advance image processing techniques such as Support Vector Machine and Artificial Neural Networks integrated with CR can be used to process the airborne hyperspectral image and generate new spectral analysis method for early detection of *Ganoderma* disease in oil palm. The new spectral analysis must also tested on other oil palm related diseases to avoid ambiguities in results.

#### 5. Acknowledgements

We would like to thanks Malaysian Palm Oil Board and University of Malaya for contribution of funding and technical assistant for this project.

#### 6. References

- [1] M.S. Arif, and A.S. Idris, “Economics of oil palm pests and *Ganoderma* disease and yield losses,” presented at the Proceedings of the 3rd MPOB-IOPRI International Seminar: Integrated Oil Palm Pests and Diseases Management, Kuala Lumpur Convention Centre, KL, November 14, 2011.
- [2] M. A. Izzuddin, “Early detection of *Ganoderma* disease in oil palm (*Elaeis guineensis* Jacq.) using field spectroscopy,” M. S. thesis, Ins. Advance. Tech., Univ. Putra Malaysia, Serdang, Malaysia, 2010.
- [3] A. S. Idris, “Basal stem rot (BSR) of oil palm (Jacq.) in Malaysia: factors associated with variation in disease severity,” Ph.D thesis, Wye College, Univ. London, Wye, United Kingdom, 1999.
- [4] C. L. Wong, J. F. C. Bong, A. S. Idris. (2012). *Ganoderma* species associated with basal stem rot disease of oil palm. *Am. J. Applied Sci.* [Online]. 9. pp. 879-885. Available:  
<http://dx.doi.org/10.3844/ajassp.2012.879.885>  
<http://thescipub.com/pdf/10.3844/ajassp.2012.879.885>
- [5] A. S. Idris, M. H. Mior, S. M. Maizatul and A. Kushairi, ”Survey on status of *Ganoderma* disease of oil palm,” presented in Proc. Int. Palm Oil Congress – Agriculture Conference, Kuala Lumpur Convention Center, KL, pp. 235-238, November 15-17, 2011.
- [6] D. Ariffin, A. S. Idris and H. Khairuddin, ”Confirmation of *Ganoderma* infected palm by drilling technique,” presented in Proc. of the 1993 PORIM International Palm Oil Congress: Update and Vision (Agriculture), Palm Oil Research Institute of Malaysia, Bangi, Selangor, pp.730-734. September 20-25, 1993.

- [7] A.S. Idris and R. Rafidah, "Enzyme linked immunosorbent assay-polyclonal antibody (ELISA-PAb)," MPOB Information Series, No. 430, 4 pp, June 2008.
- [8] A. Z. Madihah, A. S. Idris and A. R. Rafidah, " Polyclonal antibodies of *Ganoderma boninense* isolated from Malaysian oil palm for detection of basal stem rot disease," African J. Biotech. vol. 13, pp.3455-3463, August 2014.
- [9] A. S. Idris, S. Rajinder, A. Z. Madihah and M. B. Wahid, "Multiplex PCR-DNA kit for early detection and identification of *Ganoderma* species in oil palm," MPOB Information Series, No. 531, 4 pp, June 2010a.
- [10] A. S. Idris, M. S. Mazliham, P. Loonis and M. B. Wahid, "GanoSken for early detection of *Ganoderma*," MPOB Information Series, No. 499, 4 pp, June 2010b.
- [11] N. M. Nisfariza, "Early detection of *ganoderma* basal stem rot disease of oil palm by hyperspectral remote sensing," Ph.D. thesis, Univ. Nottingham, United Kingdom, 2012.
- [12] J. Zhao, D. Zhang, J. Luo, Y. Dong, H. Yang and W. Huang. (2012). Characterization of the rice canopy infested with brown spot disease using field hyperspectral data. *Wuhan Univ. J. Natural Sci.* 17.pp. 86-92. Available: <http://link.springer.com/article/10.1007/s11859-012-0809-4>
- [13] M. Zhang, Z. Qiu, X. Liu and S. L. Ustin. (2003). Detection of stress in tomatoes induced by late blight disease in California, USA, using hyperspectral remote sensing. *Int. J. App. Earth Obs. Geoinfo.* 4. pp.295-310. Available: <http://www.sciencedirect.com/science/article/pii/S0303243403000084>
- [14] H. Z. M. Shafri, M. I. Anuar, M. N. Nisfariza and A. S. Idris. (2011). Spectral discrimination of healthy and *Ganoderma*-infected oil palms from hyperspectral data. *Int. J. Rem. Sens.* 32. pp. 7111-7129. Available: <http://www.tandfonline.com/doi/abs/10.1080/01431161.2010.519003>
- [15] B. Ezzati, "Detection of *Ganoderma* basal stem rot disease using vegetation indices on hyperspectral remote sensing imagery," B. Sc. Thesis, University of Malaya, Kuala Lumpur, 2013.
- [16] J. W. Rouse, R. H. Haas, J. A. Schell, D. W. Deering and J. C. Harlan. (1974). Monitoring the vernal advancements and retrogradation (green-wave effect) of nature vegetation NASA.GSFC Final Report, Greenbelt, MD.371 pp. Available: <http://ntrs.nasa.gov/search.jsp?R=19740022555>.
- [17] D. Vaiopoulos, G. Skianis and K. Nikolakopoulos. (2004). The contribution of probability theory in assessing the efficiency of two frequently used vegetation indices, *Int. J. Rem. Sens.* 25. pp.4219-4236. Available: <http://www.tandfonline.com/doi/abs/10.1080/01431160410001680464>
- [18] A. Huete, C. Justice and J.D. Van Leeuwen. (1999). MODIS Vegetation Index (Mod 13) algorithm theoretical basis document version 3. University of Arizona, Tucson - USA.
- [19] J. E. Vogelmann, B.N. Rock and D. M. Moss. (1993). Red edge spectral measurements from sugar maple leaves. *Int. J. Rem. Sens.* 14. pp.1563-1575. Available: <http://www.tandfonline.com/doi/abs/10.1080/01431169308953986>
- [20] A. A. Gitelson, Y. Zur, B. Chickunova and M. N. Merzlyak. (2002). Assessing carotenoid content in plant leaves with reflectance spectroscopy, *Photochemical Photobiology*, 75. pp. 272-281. Available: <http://www.ncbi.nlm.nih.gov/pubmed/11950093>.
- [21] R. F. Kokaly and R. N. Clark. (1999). Spectroscopic Determination of Leaf Biochemistry Using Band-Depth Analysis of Absorption Features and Stepwise Linear Regression Remote Sensing of Environment, 67, pp.167-287.
- [22] R. Kohavi and F. Provost, On Applied Research in Machine Learning in Editorial for the Special Issue on Applications of Machine Learning and the Knowledge Discovery Process, Columbia University, N.Y.: ,1998
- [23] A. J. Viera and A. M. Garret.(2005). Understanding inter observer agreement: The kappa statistic. *Family Medic*, 37, pp. 360-360. Available: <http://www.ncbi.nlm.nih.gov/pubmed/15883903>

- [24] M. A. Cho, I. Sobhan and J. de Leeuw, "Discriminating species using hyperspectral indices at leaf and canopy scales," in Proc. The International Archives of the Photogrammetry, Remote Sensing and Spatial Information Sciences., 2008, pp. 369-376.
- [25] D. Ashourloo, M. R. Mobasheri and A. Huete. (2014). Developing two spectral disease indices for detection of wheat leaf rust (*Puccinia triticina*). *Rem. Sens.*, 6, pp.4723-4740. Available: <http://www.mdpi.com/2072-4292/6/6/4723>.
- [26] H. Z. M. Shafri and N. Hamdan. (2009). Hyperspectral imagery for mapping disease infection in oil palm plantation using vegetation indices and red edge techniques. *Am. J. Applied Sci.* [Online]. 6. pp. 1031-1035. Available: <http://thescipub.com/pdf/10.3844/ajassp.2009.1031.1035>
- [27] M. A. Izzuddin, A. S. Idris, O. Wahid, M. N. Nisfariza and H. Z. M. Shafri, "Field spectroscopy for detection of Ganoderma disease in oil palm," MPOB Information Series, No. 532, 4pp, June 2013.